Vietnam Journal of Catalysis and Adsorption
Tạp chí xúc tác và hấp phụ Việt Nam

http://chemeng.hust.edu.vn/jca/

The synthesis of γ-MnOOH nanorods as an efficient electrocatalyst for urea oxidation

Minh Tuan Nguyen Dinh,[1] Huy Thai Le,[1] Trung Hieu Le,[2] Chinh Chien Nguyen[3,4]

[1] *The University of Danang, University of Science and Technology, 54, Nguyen Luong Bang, Danang city, Viet Nam*
[2]*Faculty of Chemistry, Hue University of Sciences, Hue University, Thua Thien Hue 530000, Vietnam.*
[3] *Institute of Research and Development, Duy Tan University, Danang city 550000, Vietnam.*
[4] *Faculty of Environmental and Chemical Engineering, Duy Tan University, Da Nang 550000, Vietnam*
**Email: ndmtuan@dut.udn.vn, nguyenchinhchien@duytan.edu.vn*

ARTICLE INFO

Received: 02/3/2023
Accepted: 20/5/2023
Published: 30/6/2023

Keywords:
γ-MnOOH, urea oxidation reaction, oxygen evolution reaction

ABSTRACT

In this study, γ-MnOOH nanorods synthesized by polysaccharide- assisted hydrothermal method as an efficient electrocatalyst for urea oxidation. The γ-MnOOH structure and morphology are confirmed by X-ray diffraction and scanning electron microscopy (SEM). The γ-MnOOH material, which contains hydroxyl groups and has an average oxidation state of Mn of three as demonstrated by XPS, exhibits excellent electrocatalytic activity towards urea oxidation reaction (UOR) compared to bare nickel foam (NF). Specifically, the overpotential at 10 mA/cm^2 for γ-MnOOH is found to be 1.05 V, which is significantly lower than that of the NF (i.e., 1.12 V). Notably, the UOR over γ-MnOOH has a potential that is 180 mV lower than observed during the oxygen evolution reaction (OER) using the same electrode. These findings suggest that the γ-MnOOH nanorods could serve as a promising electro-catalyst for UOR in various energy storage and conversion applications.

Introduction

Global warming and the depletion of fossil fuels are driving humanity to explore alternative energy sources. In this context, green hydrogen has attracted distinctive attention due to its clean energy carrier, regeneration, and no pollution emissions after combustion.[1, 2] In terms of the economic aspect, green hydrogen is very potential and could be utilized as an energy source in a circular economy.[3-5]

Electrochemical water splitting has been pointed out as the most promising approach to producing green hydrogen.[6] However, the large-scale application of water electrolysis has been restricted due to its high-cost production. Such limitation originates from the oxygen evolution reaction (OER), which is a sluggish-kinetic process, involving the participation of muti-electrons. [7, 8] Consequently, an extremely high potential is required to pursue the OER at the anode side. Hence, the exploration of alternative pathways has attracted increasing consideration. To this end, electrocatalytic urea oxidation has been concerned as an interesting route for energy-saving green hydrogen generation.[9] As- a- proof-of- concept, anodic urea oxidation reaction (UOR) contains a theoretical thermodynamic potential of 0.37 Vs RHE, which is significantly lower than that of OER (1.23 Vs RHE). Furthermore, the oxidation of urea could contribute to addressing urea-polluted contaminants, a hot spot environment problem.[10] Indeed, urea is a source of nutrients for microorganisms. Wastewater containing

https://doi.org/10.51316/jca.2023.038

untreated urea can promote the growth of microorganisms. Such a phenomenon reduces water oxygen levels, which can significantly affect living organisms in the aqueous environment. In addition, the decomposition of urea can produce ammonia and CO_2, which could be a harmful substance for humans and animals.[10, 11] Hence, combining both hydrogen production and urea oxidation in a hybrid technology not only improves the efficiency of energy utilization for hydrogen production but also possesses the capability of remediating the current environmental issue.

MnOx-based electrocatalysts have been recognized as a promising candidate to carry out electrocatalytic oxidation reactions rooted in their strong oxidative capability, low cost, and environmental sustainability.[12, 13] In this context, the MnO_x phase has been considered as the primary factor, driving the catalytic performance. In particular, manganite (manganese (III) oxyhydroxide, MnOOH), a type of manganese oxide abundant trivalent Mn species, has attracted significant attention due to its unique physicochemical properties for the oxidation reaction in the aqueous phase. [14] For those reasons, numerous efforts have been devoted to explore a facile method to prepare MnOOH catalysts toward various electrocatytic applications.

Motivated by those mentioned issues, this paper reports a novel synthetic method to prepare manganese oxide-based material, targeting the electrocatalytic urea oxidation reaction. The material is prepared through a facile hydrothermal method, employing a natural polysaccharide, extracted from *Myxopyrum Smilacifolium* roots for the first time. It turns out that the existence of the polysaccharide functions as a reducing agent, maneuvering the formation of MnOOH phase, which is impossible in the conventional method. Importantly, the obtained MnOOH catalyst exhibits outstanding catalytic performance in the electrocatalytic oxidation of urea.

Experimental

Chemicals

All the chemicals were used without further purification, potassium permanganate ($KMnO_4$) was purchased from Merck. Polysaccharide was isolated and purified from *Myxopyrum Smilacifolium* roots.[15]

Pretreatment of NF

Commercial nickel foam (NF) with the dimension of 1 cm x 2 cm was carefully treated with 1M hydrochloric acid for 30 min to remove pollutants, washed with deionized water, and then cleaned with ethanol. Finally, NF was washed with deionized water and ethanol several times.

Material preparation

The MnOOH sample was synthesized by a hydrothermal method. Briefly, 0.2375 g of $KMnO_4$ and 0.1675 g of polysaccharide were dissolved in 50 mL of deionized water and vigorously stirred for 30 min. The obtained solution was then transferred into a Teflon-lined stainless-steel autoclave and hydrothermally heated at 140 ^oC for 12h. After cooling to room temperature, the product was cleaned with deionized water and ethanol several times by centrifugation and dried overnight at 65 ^oC.

Preparation of electrode

The MnOOH/NF electrode was fabricated by coating the as-prepared MnOOH on the NF surface. Typically, 5 mg of the prepared material (MnOOH) was dispersed in 1 mL of a mixed solution consisting of 970 µL ethanol and 30 µL 5 wt% Nafion solution, followed by ultrasonication for 45 min. Afterward, the resulting suspension was slowly dropped on the pretreated NF surface. The obtained electrodes were dried overnight at 65 ^oC.

Physico-chemical characterization

The crystal structure of γ-MnOOH was characterized by X-ray diffraction (SmartLab, Rigaku). The morphology was observed by a scanning electron microscope (JSM6020, JEOL). Surface properties was analyzed by x-ray photoelectron spectroscopy on PHI Quantera II apparatus using Al Kα source (1486.6 eV).

Electrochemical Measurement

The OER and UOR were conducted in a three-electrode system integrated to an electrochemical workstation (Autolab, Metrohm 101) by using γ-MnOOH- decorated NF as an anode. The working area was fixed at 2 cm^2. Ag/AgCl (3M KCl solution) and Pt plate were used as the reference electrode and counter electrode, respectively. The electrochemical electrolyte contains 1 M KOH with and without 0.33 M urea. The as-prepared electrodes were activated by

https://doi.org/10.51316/jca.2023.038

cyclic voltammetry. The polarization measurements were carried in the electrolyte of 1M KOH aqueous solution with and without 0.33 urea at the scan rate of 5 mV/s. All measured potential was converted to RHE using the formula $E_{(Vs\ RHE)} = E_{(Vs\ Ag/AgCl)} + E^0_{(Ag/AgCl)} + 0.05916 \times pH$. The polarization curves were presented without *iR* compensation. The overpotential of UOR was calculated through the formula as follows: overpotential = $E_m - E_t$, where E_m and E_t values are the measured potential vs. RHE and the theoretical value of urea oxidation reaction, which is 0.37 V.[16]

Results and discussion

The synthesis of the MnOOH catalyst is depicted in the Scheme 1. The mixture of $KMnO_4$ and isolated polysaccharide was subjected into a hydrothermal treatment to achieve the desired catalyst. In this circumstance, the polysaccharide functions as a reducing and capping agent, benefiting the formation of γ-MnOOH nanorods. Such the facile synthetic pathway has been reported for the first time.

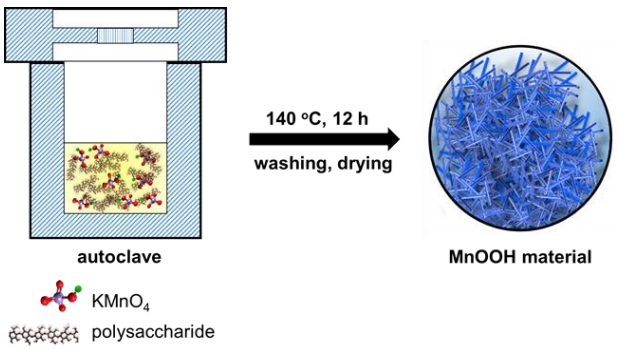

Scheme 1: The schematic illustration of γ-MnOOH nanorods

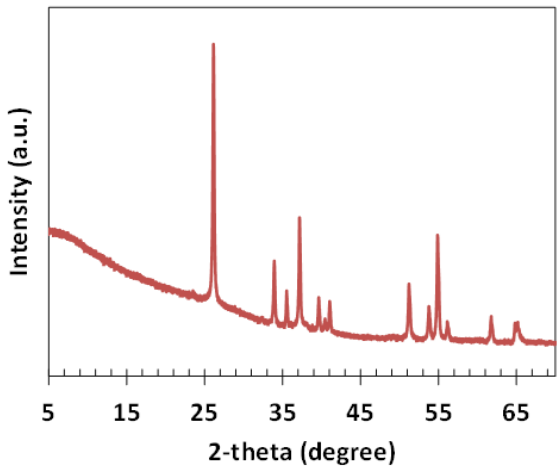

Figure 1: XRD pattern of γ-MnOOH nanorods

XRD technique is first applied to determine the crystalline phase of the obtained electrocatalysts. As shown in Figure 1, the XRD pattern of the as-prepared material shows all peaks characteristics of the monoclinic manganite phase (γ-MnOOH, ICDD PDF#088-0649), which is composed of $Mn^{3+}O_6$ octahedra linked together via their conner to form [1 × 1] octahedral chain. H^+ cations are trapped in the [1 × 1] rhombohedral tunnels. No other phase was observed, indicating that γ-MnOOH materials are successfully prepared by the redox reaction between $KMnO_4$ and polysaccharide in the hydrothermal condition at 140 °C.

The synthesized γ-MnOOH material morphology observed by scanning electron microscope indicates the formation of uniform nanorods, as depicted in Figure 2. It can be said that the nanorod morphology is typically for γ-MnOOH synthesized by the reduction of $KMnO_4$ with an appropriate amount of organic reductant in hydrothermal conditions.

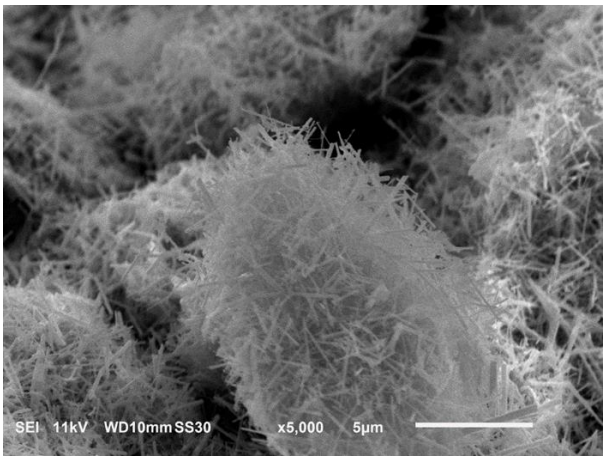

Figure 2: The SEM image of MnOOH material

The surface properties of the obtained MnOOH material are characterized by XPS. The K/Mn ratio of 0.03 indicates that a tiny portion of H cations in the 1 ×1 tunnel of the MnOOH structure is replaced by K cations or K cations are dispersed on the surface of MnOOH. The high-resolution spectra of Mn3s, Mn2p, O1s, and K2p are shown in Figure 3. Mn2p spectrum of MnOOH shows 2 peaks of $Mn2p_{3/2}$ and $Mn2p_{1/2}$ centered at 641.5 eV and 653.2 eV, respectively (Figure 3A). The $Mn2p_{3/2}$ spectrum is decomposed into multi-peaks corresponding to Mn^{2+}, Mn^{3+}, and Mn^{4+}.[17, 18]The percentages of Mn^{2+}, Mn^{3+}, and Mn^{4+} are 18.9, 62.8, and 18.3, respectively. The average oxidation state of manganese (AOS_{Mn}) of MnOOH is 3.0 respectively. The AOS_{Mn} values calculated from the orbit splitting of Mn3s are the same.

https://doi.org/10.51316/jca.2023.038

O1s spectra show three components of lattice oxygen (O_I), surface-adsorbed oxygen species (O_{II}), and hydroxyl-based species (O_{III}) at 529.5 eV, 531.0 eV, and 532.0 eV, respectively. The atomic ratio of O_{II}/O_I and O_{III}/O_I are 0.3 and 0.29, respectively for MnOOH. The high percentage of O_{III} in the MnOOH sample is consistent with the existence of hydroxyl groups linked to the MnO_6 octahedra via oxygen atoms in the manganite structure. Such a high O_{III}/O_I ratio could enhance the conductivity of the sample and improve the electrocatalytic activity of the MnOOH electrocatalysts.

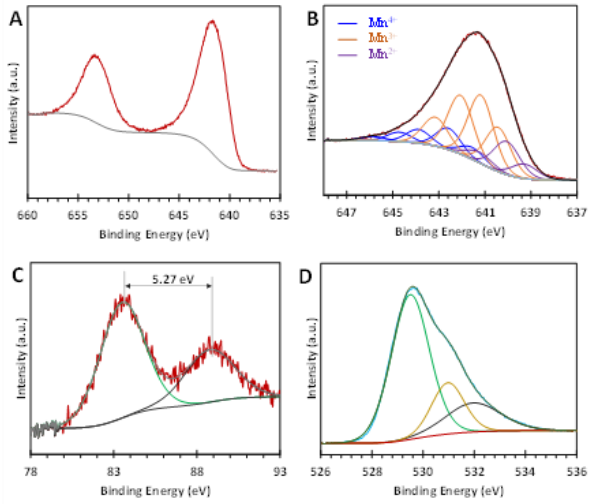

Figure 3: XPS spectra of MnOOH sample A) Mn3s, B) Mn2p, C) Decomposition of $Mn2p_{3/2}$, and D) O1s

The electrochemical UOR performance of the as-prepared γ-MnOOH was examined and compared to that of nickel foam (NF) electrodes. In this work, the urea solution of 0.33 M, which is close to the urea concentration in human urine, is opted. The electrocatalytic performances of the γ-MnOOH electrode for the UOR and OER are firstly evaluated by linear sweep voltammetry (LSV) in an alkaline medium (KOH; pH=14) with and without urea, respectively, as shown in Figure 4A. The γ-MnOOH- containing electrode, performing UOR, requires a potential of 1.42V to achieve a current density of 10 mA/cm^2, which is 180 mV lower than that of OER (i.e., 1.6V vs RHE). Furthermore, the LSV curves of the γ-MnOOH and bare NF electrodes obtained in the 1M KOH and 0.33 M urea solution were also carried out, as depicted in Figure 4B.

The γ-MnOOH sample outperforms the bare NF, suggesting the significance of the γ-MnOOH material to drive the oxidation reaction of urea. Such evidence highlights the outstanding capability of the γ-MnOOH catalysts toward energy-saving H_2 production in comparison to the conventional electrolysis of water.

To explore the reaction kinetics of these catalysts, the Tafel slopes derived from corresponding UOR polarization, as shown in Figure 4C. The catalytic performance and charge transfer kinetics are directly proportional to the Tafel slope. In other words, a lower Tafel slope suggests an improved performance and faster charge transfer kinetics. The γ-MnOOH/NF deposited electrode possesses a Tafel slope of 27.4 mV dec^{-1}, which is smaller than that of NF (i.e., 40.4 mV dec^{-1}), suggesting the fast electron transfer rate and superior UOR catalytic kinetics. At 10 mA/cm^2, the overpotential over the γ-MnOOH anode is 1.05 V, much lower than Nickel foam, indicating the best electro-catalytic performance of γ- MnOOH for UOR, as displayed in Figure 4D. It can be said that using γ-MnOOH as electrode material significantly improves the electrocatalytic activity of the oxidation of urea at the anode.

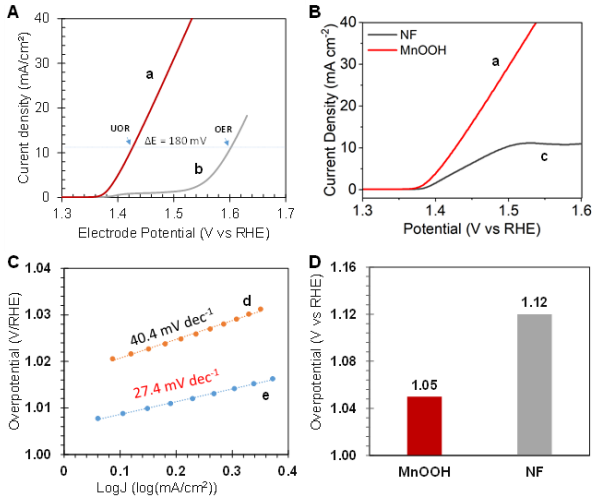

Figure 4: A) LSV curve over γ-MnOOH electrode for (a) UOR and (b) OER; B) LSV curve over (a) MnOOH, (c) NF electrodes for UOR at the scanning rate of 5mV/s; C) Tafel plot of (d) NF and (e) MnOOH electrode; and D) Overpotential at 10 mA/cm2 over MnOOH and NF electrodes

Conclusion

In conclusion, γ-MnOOH nanorods electro-catalyst are successfully synthesized through a facile hydrothermal redox method using polysaccharide as a reducing agent. The resulting material shows the excellent electrocatalytic activity as an anode for the urea oxidation reaction (UOR). Thus, the UOR over γ-MnOOH-based material exhibits a remarkably low potential oxygen evolution reaction (OER) using the same electrode. Moreover, the prepared γ-MnOOH-

https://doi.org/10.51316/jca.2023.038

decorated anode delivers an overpotential of 1.05 V at 10 mA/cm^2, which was significantly lower than that of bare nickel foam. Such evidence suggests that γ-MnOOH nanorods could serve as a promising electrocatalyst for UOR for energy-saving hydrogen production. Furthermore, the synthesis method presented in this study offers a facile and environmentally friendly approach for the preparation of efficient and cost-effective electro-catalysts, which could be extended to other electrochemical systems beyond UOR. Overall, this work provides a significant step towards the development of highly active and stable electro-catalysts for various renewable energy applications.

Acknowledgments

This research is funded by Kurita Water and Environment Foundation (KWEF) under grant number 22Pvn051-T5

References

1. M. Momirlan, T.N. Veziroglu, Renewable and Sustainable Energy Reviews, 6 (2002) 141-179. https://doi.org/10.1016/S1364-0321(02)00004-7
2. A. Midilli, M. Ay, I. Dincer, M.A. Rosen, Renewable and sustainable energy reviews, 9 (2005) 255-271. https://doi.org/10.1016/j.rser.2004.05.003
3. E.I. Zoulias, N. Lymberopoulos, Renewable Energy, 32 (2007) 680-696. https://doi.org/10.1016/j.renene.2006.02.005
4. Z. Fan, E. Ochu, S. Braverman, Y. Lou, G. Smith, A. Bhardwaj, J. Brouwer, C. McCormick, J. Friedmann, Columbia Center for Global Energy Policy, (2021).
5. M. Yáñez, A. Ortiz, B. Brunaud, I.E. Grossmann, I. Ortiz, Computer Aided Chemical Engineering, Elsevier (2019) 1777-1782. https://doi.org/10.1016/B978-0-12-818634-3.50297-6
6. M.F. Lagadec, A. Grimaud, Nature Materials, 19 (2020) 1140-1150. https://doi.org/10.1038/s41563-020-0788-3
7. D. Hyung Kweon, I.-Y. Jeon, J.-B. Baek, Advanced Energy and Sustainability Research, 2 (2021) 2100019. https://doi.org/10.1002/aesr.202100019
8. Y. Liang, K. Banjac, K. Martin, N. Zigon, S. Lee, N. Vanthuyne, F.A. Garcés-Pineda, J.R. Galán-Mascarós, X. Hu, N. Avarvari, M. Lingenfelder, Nature Communications, 13 (2022) 3356. https://doi.org/10.1038/s41467-022-31096-8
9. D. Zhu, H. Zhang, J. Miao, F. Hu, L. Wang, Y. Tang, M. Qiao, C. Guo, Journal of Materials Chemistry A, 10 (2022) 3296-3313. https://doi.org/10.1039/D1TA09989B
10. J. Li, S. Wang, J. Chang, L. Feng, Advanced Powder Materials, 1 (2022) 100030. https://doi.org/10.1016/j.apmate.2022.01.003
11. W. Sun, J. Li, W. Gao, L. Kang, F. Lei, J. Xie, Chemical Communications, 58 (2022) 2430-2442. https://doi.org/10.1039/D1CC06290E
12. H. Zhang, Y. Bai, X. Lu, L. Wang, Y. Zou, Y. Tang, D. Zhu, Inorganic Chemistry, (2023). https://doi.org/10.1021/acs.inorgchem.3c00234
13. K.S. Bhavani, T. Anusha, P.K. Brahman, Electrochimica Acta, 399 (2021) 139394. https://doi.org/10.1016/j.electacta.2021.139394
14. C. Walter, S. Kalra, R. Beltrán-Suito, M. Schwarze, P.W. Menezes, M. Driess, Materials Today Chemistry, 24 (2022) 100905. https://doi.org/10.1016/j.mtchem.2022.100905
15. T.H. Le, L.S. Le, D.G.C. Nguyen, T.V.T. Tran, X.A. Vu Ho, T.M. Tran, M.N. Nguyen, V.T. Nguyen, T.T. Le, T.H.C. Nguyen, C.C. Nguyen, Q.V. Le, ACS Omega, 7 (2022) 47923-47932. https://doi.org/10.1021/acsomega.2c05779
16. K. Li, Y. Tong, ChemCatChem, 14 (2022) e202201047. https://doi.org/10.1002/cctc.202201047
17. M.C. Biesinger, B.P. Payne, A.P. Grosvenor, L.W.M. Lau, A.R. Gerson, R.S.C. Smart, Applied Surface Science, 257 (2011) 2717-2730. https://doi.org/10.1016/j.apsusc.2010.10.051
18. M.T. Nguyen Dinh, C.C. Nguyen, T.L. Truong Vu, V.T. Ho, Q.D. Truong, Applied Catalysis A: General, 595 (2020) 117473. https://doi.org/10.1016/j.apcata.2020.117473